Airfoil design: Finding the balance between design lift and structural stiffness

Bak, Christian; Gaudern, Nicholas; Zahle, Frederik; Vronsky, Tomas

Published in:
Journal of Physics: Conference Series (Online)

Link to article, DOI:
10.1088/1742-6596/524/1/012017

Publication date:
2014

Document Version
Publisher's PDF, also known as Version of record

Airfoil design: Finding the balance between design lift and structural stiffness

2014 J. Phys.: Conf. Ser. 524 012017

(http://iopscience.iop.org/1742-6596/524/1/012017)

Airfoil design: Finding the balance between design lift and structural stiffness

Christian Bak[1], Nicholas Gaudern[2], Frederik Zahle[1], Tomas Vronsky[2]
DTU Wind Energy, DTU Risø Campus
Frederiksborgvej 399, 4000 Roskilde, Denmark

E-mail: chba@dtu.dk

Abstract. When upscaling wind turbine blades there is an increasing need for high levels of structural efficiency. In this paper the relationships between the aerodynamic characteristics; design lift and lift-drag ratio; and the structural characteristics were investigated. Using a unified optimization setup, airfoils were designed with relative thicknesses between 18% and 36%, a structural box height of 85% of the relative thickness, and varying box widths in chordwise direction between 20% and 40% of the chord length. The results from these airfoil designs showed that for a given flapwise stiffness, the design lift coefficient increases if the box length reduces and at the same time the relative thickness increases.

Even though the conclusions are specific to the airfoil design approach used, the study indicated that an increased design lift required slightly higher relative thickness compared to airfoils with lower design lift to maintain the flapwise stiffness. Also, the study indicated that the lift-drag ratio as a function of flapwise stiffness was relatively independent of the airfoil design with a tendency that the lift-drag ratio decreased for large box lengths.

The above conclusions were supported by an analysis of the three airfoil families Risø-C2, DU and FFA, where the lift-drag ratio as a function of flapwise stiffness was decreasing, but relatively independent of the airfoil design, and the design lift coefficient was varying depending on the design philosophy. To make the analysis complete also design lift and lift-drag ratio as a function of edgewise and torsional stiffness were shown.

1. Introduction

Since the late 1970s there has been a continuous upscaling of wind turbines. Linear scaling causes a challenge because the mass of the blade increases with the cube of the length. The largest wind turbines on the market or in development have a rating in the order of 8 MW; however, increasing the size further will be even more challenging.

When upscaling wind turbine blades there is an increasing need for high levels of structural efficiency to control blade mass and limit deflection. Using thick airfoils will stiffen the blade, but this will in general reduce the aerodynamic efficiency. On the other hand the use of thinner airfoils will in general increase the aerodynamic efficiency, but the stiffness will be low. When investigating wind turbine blade shapes, they vary in general from manufacturer to manufacturer: some blades are rather wide and others are very slender. These differences depend on the choice of both design lift and design tip speed ratio. Wind turbine blades can either use airfoils designed by research institutes [1,2,3,4,5] or manufacturers that are specific to wind turbines, or use airfoils dedicated the aviation industry [6].

[1] DTU Wind Energy
[2] Vestas Wind Systems A/S

Optimizing the aerodynamic performance and the blade weight will require further investigation of the correlation between stiffness and aerodynamic performance.

Airfoil designs are in general very different; even though two airfoils show the same maximum lift, the shape can be very different. The reason is that the airfoil shape depends on many parameters, such as the requirements for maximum lift, the position of the transition from laminar to turbulent flow, structural stiffness and the Reynolds number. As a result, there are many potential airfoil shapes that can fulfil the requirement for e.g. a certain maximum lift. Even though there is not an unambiguous relation between e.g. the requirement for maximum lift and the airfoil shape, an investigation is needed to highlight the relationship between aerodynamic performance and structural stiffness.

In this work the relationship between design lift, lift-drag ratio and structural stiffness is mapped. This mapping indicates the tradeoff between achieving structural stiffness through the use of a larger internal space in the airfoil or by a larger relative thickness. Using a similar design method as for the Risø-C2 family [2], a number of airfoil families ranging from a relative thickness of 18% to 36% are designed, where the aerodynamic objectives and constraints are similar, but where the structural constraints change. Thus, the space in the internal part of the airfoil was varied from airfoil to airfoil. Since the airfoil shapes in general were very different and since each airfoil was only designed to a draft level, the current study should be considered as a trend study rather than a search for the exact design lift coefficient and corresponding stiffness.

2. Airfoil design method

Airfoils with four different relative thicknesses were designed, t_{max}/c=18%, 24%, 30% and 36% and for each of these thicknesses the requirements for internal space in the airfoils were increased to investigate how $c_{l,max}$ and c_l-c_d ratio correlate to the structural constraints.

The airfoil design tool, AirfoilOpt, is a 2D design tool and has been used to design previous Risø airfoil families [1,2]. It uses a direct method where numerical optimization is coupled with the flow solver, which is a panel code with inviscid/viscous interaction. A number of design variables form the airfoil shape, which is optimized subject to design objectives and constraints. Direct methods, such as the method used, are basically interdisciplinary and multi-point and they allow direct use of integrated response parameters such as airfoil c_l and c_d as design objectives. In addition, boundary layer response parameters, e.g., skin friction and transition point location can be constrained or used as objectives. Structural characteristics can be controlled by constraining the shape in terms of coordinates, gradients, curvatures or moment of resistance.

2.1. Design algorithm

Subject to constraints, the design variables are changed in an optimization problem to minimize the objective function; in this case the design variables are the control points that describe the airfoil shape. The constraints are the side values for the design variables and the bounds on response parameters from the flow and structural calculations. A traditional Simplex optimizer was used with a finite difference sensitivity analysis. This is a simple and robust solution method; however, it is computationally expensive because of the large number of necessary flow calculations. The optimization process is iterative involving numerous calculations of flow and structural response parameters where the design gradually changes to improve the objective. The calculated flow and structural response parameters are used to estimate the value of the objective function and the constraints. Multiple angles of attack are calculated to allow off-design optimizations. The combination of flow and structural responses allows multidisciplinary optimization (MDO).

2.2. Geometry description

A smooth shape is important for the optimization results. The 2D airfoil shape was represented by a single B-spline defined from the trailing edge around the airfoil contour by a set of control points. The blade shape was represented by cubic B-splines fixed at the top and bottom of the 2D sections and at

the leading and trailing edges. In between these four fixed points on the sections the splines were distributed evenly along the surface length.

2.3. Flow analysis

The XFOIL code ver 6.1 was used for the flow calculations during the optimization, Drela [7]. For a given *AOA* and *Re*, XFOIL provides the c_p-distribution, c_l, and c_d. In addition, numerous boundary layer parameters are calculated. Transition was modeled by the e^n method with n = 9. Prescribing transition to x/c=0.001 after the leading edge on the suction side and at x/c=0.10 after the leading edge on the pressure side simulated leading edge roughness. XFOIL is well suited for optimization because of the fast and robust viscid/in-viscid interaction scheme; however, the integral boundary layer formulation is not well suited for separated flows. XFOIL should therefore be used with caution at and above $c_{l,max}$.

3. Strategy for airfoil design

The desirable airfoil characteristics form a complex matrix of properties, some of which are in conflict with each other. This has been a topic of discussion in the literature, Tangler [4], Björk [8], Fuglsang [9]. There seems to be consensus on most of the general desirable characteristics; however, the means of achieving them are strongly related to the design method and the philosophy of the designer. The new airfoils were designed for operation on a wind turbine rotor. The force that contributes to the rotor power is the tangential force, whereas the force that contributes to the rotor thrust, is the normal force. As it was the case with the Risø-B1 airfoil family the tangential force coefficient can be used as the objective function, but also the lift-drag ratio, c_l/c_d, can be used as it was the case with the Risø-C2 airfoil family. The latter is a common measure of the airfoil efficiency because c_l can be considered as the production and c_d can be considered as the loss. The airfoils created in this work were designed with maximum c_l-c_d ratio.

Figure 1 shows in terms of c_l vs. *AOA* the different characteristics that are taken into account in the design process. Some of the characteristics will be described in the following sections.

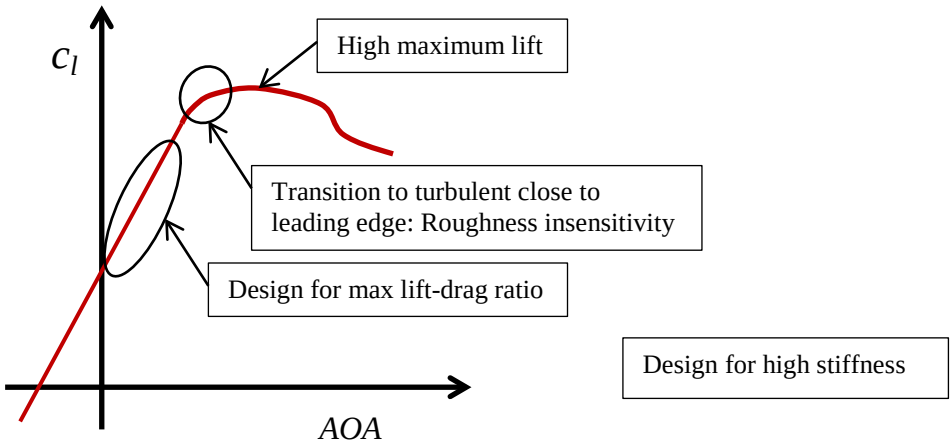

Figure 1 Sketch of the design strategy for wind turbine airfoils.

The designs of the airfoils shown in this paper were based on the same objective function and constraints for all airfoils, apart from the constraints that scale with the relative thickness. Compared to the design process in this work, an airfoil design process targeting airfoils ready for use on wind turbine rotors would require more emphasis on further optimization of details in the aerodynamics and/or the structure. Thus, the airfoils are designed to a draft level.

3.1. Structure

A wind turbine blade may be divided into the root, mid, and tip sections. The mid and tip sections are determined mainly from aerodynamic requirements whereas the inboard section of the blade is more driven by structural objectives. The relative thickness, t_{max}/c ratio, is the most important parameter; also important are the location of the maximum thickness on the chord and the local shape of the airfoil. Thus, in the design of the airfoils, the relative thickness was constrained at x/c=0.15 and between x/c=0.35 and x/c=0.60 (depending on t_{max}/c), to be at least 0.85 times t_{max}/c. This formed a space within the airfoil allowing for more or less distance between the sparcaps.

Because of the possibility of high $c_{l,max}$ significant camber was allowed on the pressure side. The thickness of the trailing edge was kept finite, but thin (appr. 2.5% of the relative thickness) to minimize trailing edge noise.

3.2. Insensitivity of $c_{l,max}$ to leading edge roughness

Roughness on the airfoil leading edge region formed by the accumulation of dust, dirt and bugs or erosion is well recognized as a key design driver for wind turbine airfoils [2,10]. The airfoils in this study were designed for minimum sensitivity of $c_{l,max}$ to leading edge roughness by using two separate design objectives. Firstly, the suction side natural transition point was constrained to move to the very leading edge for *AOA* a few degrees below $c_{l,max}$ predicted with forced transition. This determined the local shape of the leading edge region so that a small pressure rise at the leading edge caused natural transition to turbulent flow at the leading edge a few degrees before $c_{l,max}$. Premature transition caused by roughness will therefore be eliminated close to $c_{l,max}$ by a very forward position of the natural transition point. Secondly, the value of $c_{l,max}$ resulting from a flow analysis with simulation of leading edge roughness, i.e. forced transition from the very leading edge, was constrained to be sufficiently high compared to results from analysis assuming free transition. This shapes the airfoil suction side so that the pressure recovery region does not separate prematurely due to an increase of the boundary layer thickness caused by roughness, which would reduce $c_{l,max}$. Even with this constraint large amounts of roughness will inevitably reduce $c_{l,max}$. The existence of even minor leading edge roughness will result in an unavoidable reduction in the c_l-c_d ratio, because the existence of leading edge roughness will make the laminar boundary layer less stable and cause earlier transition to a turbulent boundary layer causing an increase in drag.

3.3. Design $c_{l,max}$

The airfoil sections were designed for the highest $c_{l,max}$ possible, given the geometric constraints. This was chosen because the airfoil sections can be used to design as slender blades as possible, which in general helps to reduce fatigue loads and extreme loads [11]. Also, no matter which concept is used in the blade design, the inner part of the rotor needs airfoil sections with both high relative thickness and high maximum lift.

3.4. Design objective

A compound objective function was defined as a weighted sum of c_l-c_d ratio values resulting from multiple angles of attack in the design *AOA* range. Some were for a clean airfoil surface whereas others were for flow with simulated leading edge roughness to ensure good performance at both conditions. The airfoil design *AOA*-region is also determined from the requirements for the wind turbine off-design operation. Due to the stochastic nature of the wind, turbulent gusts and wind direction changes will always lead to some off-design operation due to non-uniform inflow; however, the degree of off-design operation is mainly driven by the power control principle. In most cases it is desirable that the design *AOA*-region is close to $c_{l,max}$ since this enables low rotor solidity and/or low rotor speed. For all the new airfoils in this study the design point region was $AOA_r \in [6°; 14°]$, where AOA_r is the angle of attack relative to $AOA@(c_l=0)$. This should lead to an expected high $c_{l,max}$. The airfoils were designed for Re=9x10^6, because this corresponds to modern blade designs of the 6MW size.

4. Structural evaluation

To evaluate the airfoils structurally, stiffness was mapped. The challenge of this mapping was to make it as realistic and fair as possible, but at the same time the method had to be simple to facilitate the fast evaluation of many airfoils. In blade design the airfoil chord length corresponds to the chosen design lift; this is because the thrust of the rotor should be kept constant, and as a result lift, $L_{design}=0.5*\rho*V^2*c*c_{l,design}$, needs to be kept constant. Here L_{design} is the design lift, ρ is the air density, V is the relative velocity, c is the chord length and $c_{l,design}$ is the design lift coefficient. Thus, assuming constant velocity, $c*c_{l,design}$ needs to be kept constant. The chosen design strategy was to:

- calculate the design lift coefficient by subtracting 0.45 from the maximum lift coefficient (assuming forced transition from the leading edge). This value was chosen to ensure a reserve if a turbulent gust appear, when the rotor operates close to rated power, so that the airfoil does not enter stall. The value could be slightly different, depending on the turbine control.
- scale the chord in accordance to the design lift e.g. with a reference design lift of 1 (one) and reference chord length of 1 (one). The chord was computed to be $1/c_{l,design}$.
- keep a constant % chord spar width (so width scales with chord). The sparcap width was chosen to be 25% for all airfoils.
- modify the spar thickness so that the spar area (and hence mass) was the same for all airfoils.
- position the spar in the optimal position for flapwise stiffness i.e. largest coverage of the thickest part of the airfoil.

An example of a structural layout is seen in Figure 2. When evaluating each airfoil in the same t_{max}/c family, the following structural parameters were kept constant:

- thickness of LE and TE core material
- thickness of spar webs
- thickness and dimensions of TE reinforcement

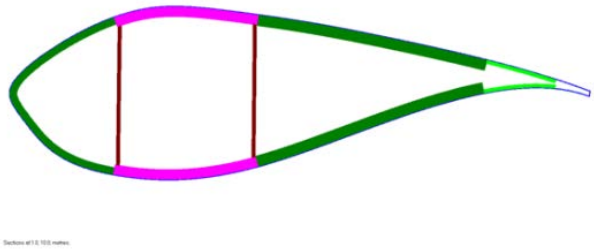

Figure 2 An example of a structural layup of a 30% airfoil

In the evaluation process it was intended to keep the mass identical for all airfoils; to give consistency to the structural design, and to keep the methodology simple this was not achieved. When the airfoil shape or chord are changed, the structural section mass also changes despite the parametric layup remaining constant (due to area differences). These small shape changes are unlikely to have a significant impact on structural characteristics such as web shear strains and panel buckling margins; therefore without carrying out detailed load/structural analysis it does not make sense to alter glass and core thicknesses to try to keep section mass constant between airfoils. Sensible thicknesses and dimensions were chosen, and maintained. To minimize any bias in the results due to section mass, the stiffness relative to the mass was used as the relevant parameter for analysis.

A proprietary structural analysis program used for initial blade design was used to calculate the structural section properties. The program is based on two-dimensional Euler beam theory. Composite material properties are pre-calculated and provided as input data. The program takes normalized airfoil shape data and scales it to the desired chord and t_{max}/c ratio, datum lines are then defined to aid in the positioning of the internal layup. Materials are assigned to their relevant zones before the entire section was discretized around its perimeter. The discretized profile was then used to calculate all sectional mass and stiffness properties.

5. Results

5.1. The airfoil designs

An example of the airfoil designs are seen in Figure 3 reflecting the 30% airfoil thickness designed with the different constraints on the airfoil's internal space. It is noted how the internal space constraints affect the overall airfoil shape. A high degree of camber is seen close to the trailing edge to obtain as high $c_{l,max}$ as possible. It should be noted that the sparcap for the airfoil with the "25% box" is much thicker than on the airfoil with the "37.5% box". The reason is that the "25% box" airfoil has higher design lift coefficient that results in a smaller chord proportional to $1/c_{l,design}$; the "37.5%" box airfoil has a much bigger chord because of the lower design lift coefficient. Finally, these airfoil designs are not considered as "ready for wind tunnel tests", but more as a first draft in the airfoil design process.

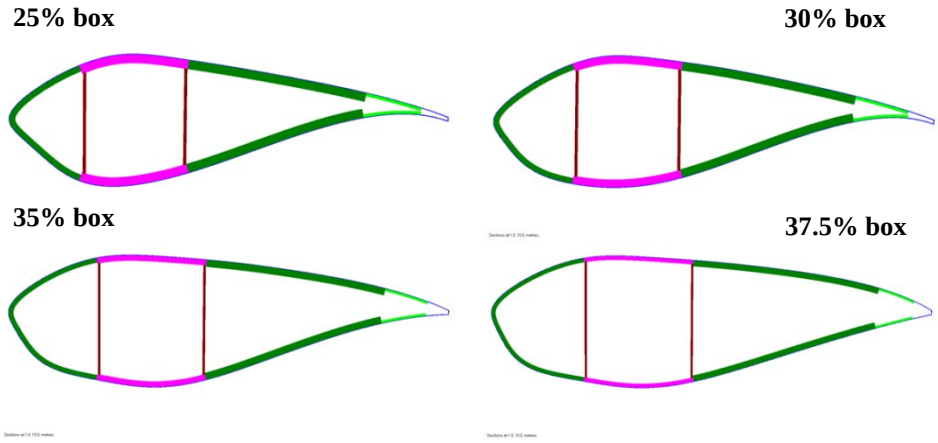

Figure 3 An example of the designs and the structural layup of selected 30% airfoils.

5.2. The aerodynamic and structural evaluation

In Table 1 the key aerodynamic and structural parameters are shown. The aerodynamic characteristics are based on transition forced at x/c=0.001 on the suction side and x/c=0.1 on the pressure side and with Reynolds number, Re=9x10^6. The design lift, $c_{l,design}$, is defined as $c_{l,max}$-0.45 and the lift-drag ratio, c_l/c_d, is evaluated at $c_{l,design}$. Also, the local power coefficient loss was predicted relative to inviscid flow at a local speed ratio, $\lambda_{local}=\omega r/U$ =7, using the formula stated by Bak [12]: $CP_{local,loss}=\frac{3}{2}\frac{\lambda_{local}}{c_l/c_d}$, where ω is the rotational speed [rad/s], r is the radius of interest [m] and U is the wind speed [m/s]. To indicate the quality of the airfoil designs, they are compared to existing airfoils, see Figure 4. With the chosen existing airfoils, both the new airfoils and the existing airfoils follow the same trend.

The key parameters shown in Table 1 are plotted in Figure 5, and alternatively in Figure 6. The points at the very left in the plots of Figure 6 show the characteristics of the 18% airfoils, whereas the points at the very right are from the 36% airfoils. The left hand plot shows that the shorter the box length is, the higher the design lift that can be obtained for a given flapwise stiffness. It also shows that the flapwise stiffness for a certain relative thickness is reduced if higher design lift is required; however, a certain stiffness can be obtained if a higher relative thickness is selected. The right hand plot shows that the lift-drag ratio is relatively independent of whether increased stiffness is obtained by either increased box length or increased relative thickness, but with the tendency that the lift-drag ratio is slightly lower if the box length is large. Thus, for box lengths greater than 30% to 35% the lift-drag ratio is slightly lower.

Table 1 Aerodynamic and structural key parameters.

Box length [%]	t/c [-]	$C_{l,max}$ [-]	$C_{l,design}$ [-]	c_l/c_d [-]	Local CP loss [%]	Chord length [m]	EI_{flap}/m [N/m^2/kg]
20	**18**	2.06	1.61	114.9	9.1	0.620	67.9E+03
20	**24**	1.84	1.39	99.5	10.6	0.721	161E+03
25	**18**	1.96	1.51	112.9	9.3	0.661	69.6E+03
25	**24**	1.84	1.39	98.7	10.6	0.718	173E+03
25	**30**	1.71	1.26	83.0	12.7	0.796	328E+03
25	**36**	1.62	1.17	65.0	16.1	0.857	537E+03
30	**18**	2.01	1.56	113.9	9.2	0.643	71.2E+03
30	**24**	1.84	1.39	97.6	10.8	0.722	179E+03
30	**30**	1.63	1.18	78.7	13.3	0.850	372E+03
30	**36**	1.50	1.05	60.4	17.4	0.949	645E+03
35	**18**	2.01	1.56	110.4	9.5	0.641	76.8E+03
35	**24**	1.76	1.31	92.9	11.3	0.762	199E+03
35	**30**	1.43	0.98	64.4	16.3	1.023	514E+03
35	**36**	1.46	1.01	48.7	21.6	0.991	676E+03
37.5	**30**	1.27	0.82	53.0	19.8	1.213	687E+03
37.5	**36**	1.30	0.85	42.3	24.8	1.172	902E+03
40	**18**	1.98	1.53	103.6	10.1	0.655	82.3E+03
40	**24**	1.61	1.16	81.6	12.9	0.863	249E+03

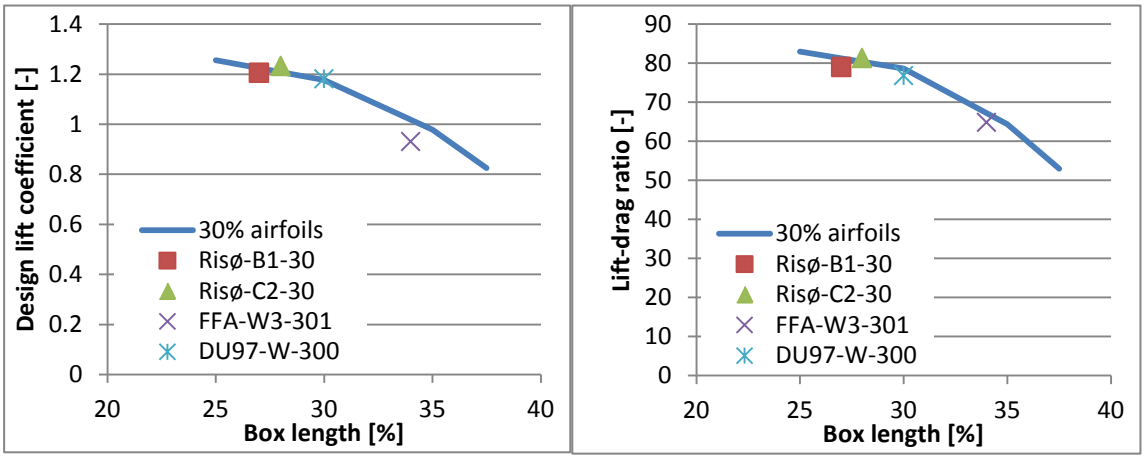

Figure 4 The 30% aerodynamic airfoil characteristics as a function of box length compared to existing airfoils with same relative thickness.

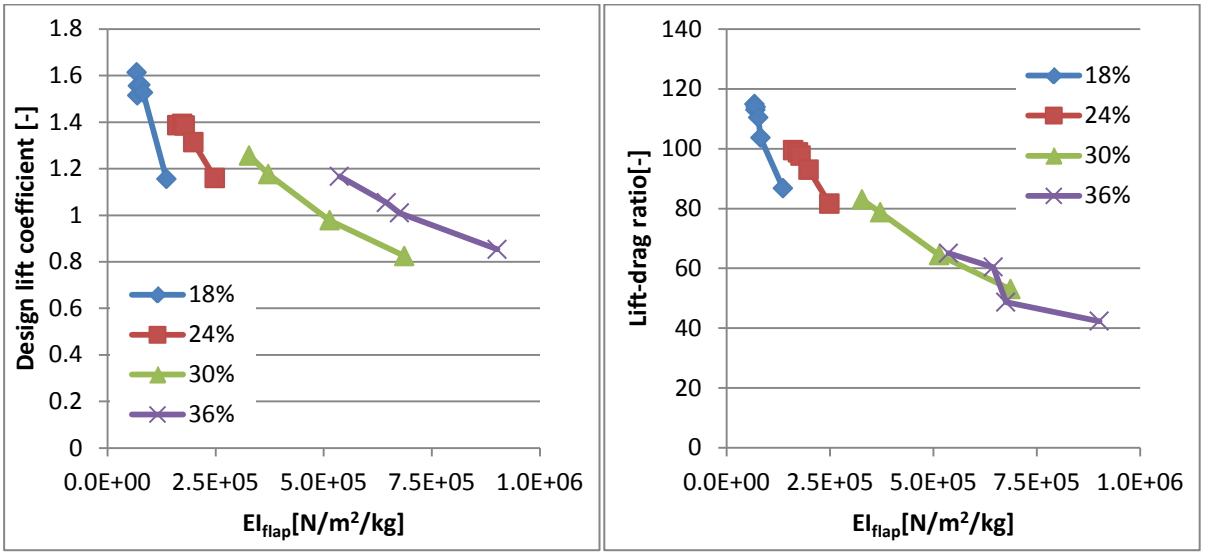

Figure 5 Left: Design lift coefficient as a function of flapwise stiffness per mass, EI_{flap} , Right: Lift-drag ratio as a function of flapwise stiffness per mass, EI_{flap}.

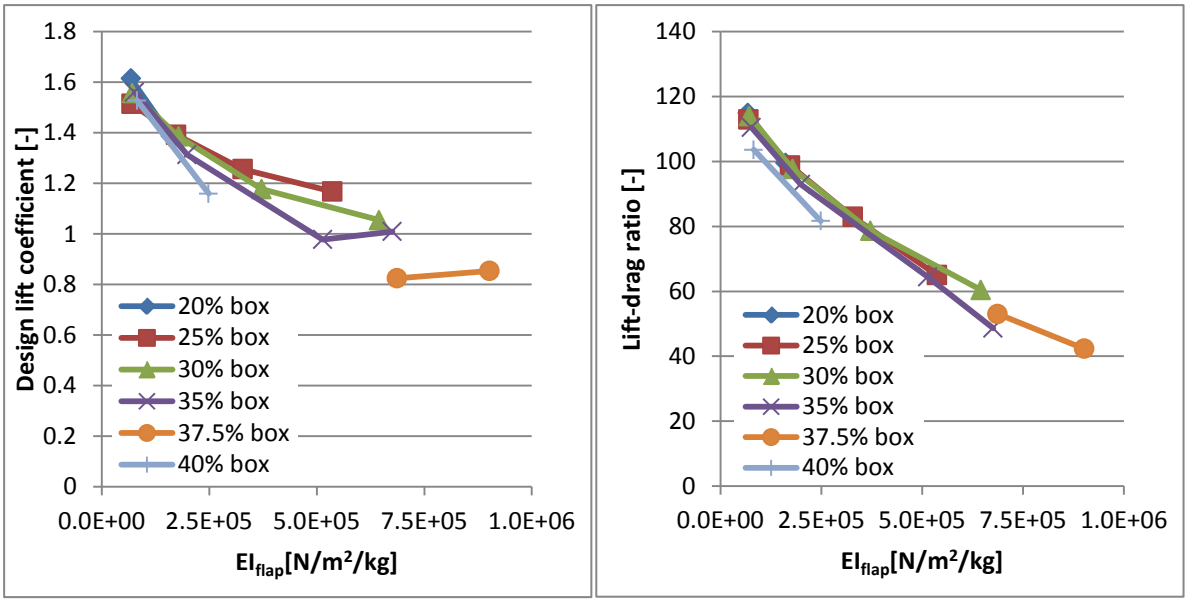

Figure 6 Left: Design lift coefficient as a function of flapwise stiffness per mass, EI_{flap}. Right: Lift-drag ratio as a function of flapwise stiffness per mass, EI_{flap}.

To further investigate the trends shown in Figure 6, three existing airfoil families are analyzed in a unified way as above and shown in Figure 7:

- Risø-C2 (Risø-C2-18, Risø-C2-21, Risø-C2-24, Risø-C2-30 and Risø-C2-36) with relatively high camber and corresponding small box size (28-31%),
- DU (DU96-W-180, DU91-W2-250, DU97-W-300 and DU00-W2-350) with a camber less than the Risø-C2 airfoil family and corresponding larger box size (30-36%), especially for the smaller relative thicknesses and
- FFA (FFA-W3-211, FFA-W3-241, FFA-W3-301, FFA-W3-360) also with a camber less than the Risø-C2 airfoil family and corresponding larger box size (31-35%).

The analysis showed that the lift-drag ratio as function of flapwise stiffness was the same for the three airfoil families, which was the same conclusion made based on Figure 6. However, the trend for the design lift as a function of flapwise stiffness was less clear, where especially the thinnest DU and FFA airfoils show significantly lower design lift than the Risø-C2 airfoil. This deviation was possibly intended, since an airfoil with relatively low lift could have been the target in the design of the airfoil families in contrast to the Risø-C2-18 to -24. It should also be noted that the Risø-C2-24 airfoil had approximately the same flapwise stiffness as the DU-W-180 and FFA-W3-211 airfoils, but also that the lift-drag ratio was the same for all three airfoils, however with a design lift at appr. 1.4 for the Risø-C2 airfoil and appr. 1.25 for the DU and FFA airfoils. The comparisons between the existing airfoils lead therefore to the same conclusion as above; that flapwise stiffness can be obtained either by increasing relative thickness or increasing box length.

To complete the analysis, also the edgewise stiffness and torsional stiffness were included in the plots. It showed that the lift-drag ratio not always was inversely proportional to the edgewise stiffness, where the DU and FFA airfoils seem to have similar edgewise stiffness for different relative thicknesses. It also showed that the torsional stiffness followed the same trend as the flapwise stiffness, however with stiffness values that were approximately 10 times lower.

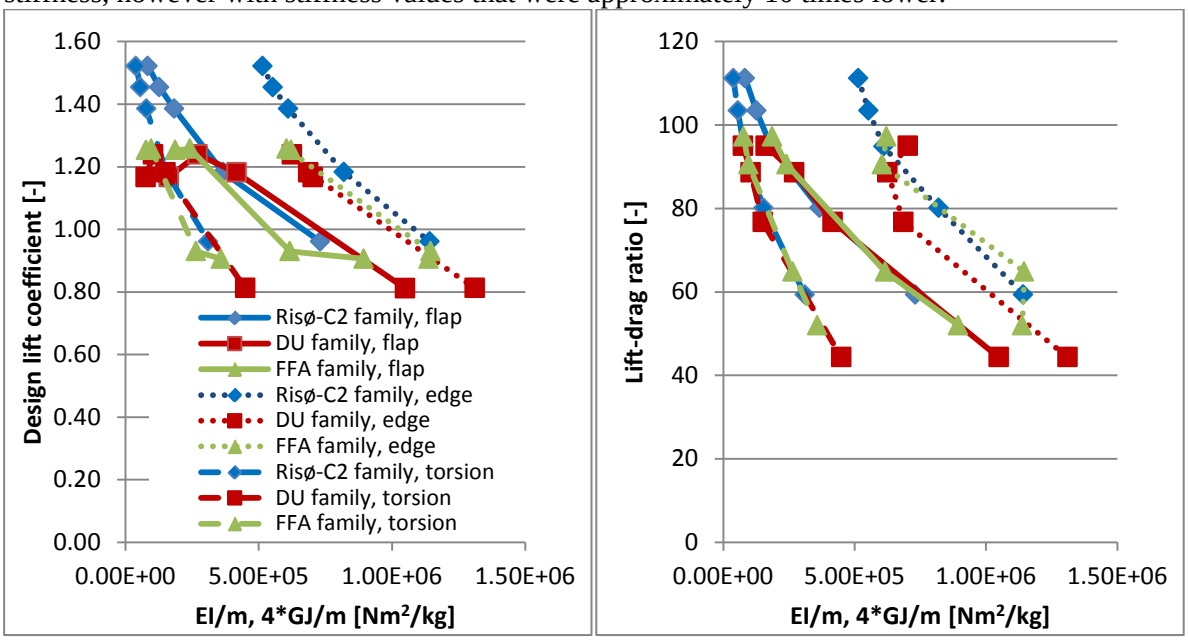

Figure 7 Left: Design lift coefficient as a function of stiffness per mass, *EI* and *GJ*. Right: Lift-drag ratio as a function of stiffness per mass, *EI* and *GJ*.

6. Conclusion

When upscaling wind turbine blades there is an increasing need for high levels of structural efficiency. In this paper the relationships between the aerodynamic characteristics; design lift and lift-drag ratio; and the structural characteristics were investigated. Using a unified optimization setup, airfoils were designed with relative thicknesses between 18% and 36%, a structural box height of 85% of the relative thickness, and varying box widths in chordwise direction between 20% and 40% of the chord. The structural architecture is unified and takes into account the difference in chord length according to the design lift coefficient. The results from these airfoil designs showed that for a given flapwise stiffness, the design lift coefficient increases if the box length reduces and at the same time the relative thickness increases.

Even though the conclusions are specific to the airfoil design approach used, the study indicated that an increased design lift required slightly higher relative thickness compared to airfoils with lower design lift to maintain the flapwise stiffness. Also, the study indicated that the lift-drag ratio was

decreasing for increasing flapwise stiffness, but relatively independent of airfoil design philosophy, however with a tendency that the lift-drag ratio decreased for larger box lengths.

These conclusions were supported by an analysis of the existing Risø-C2, DU and FFA airfoil families that reflected the same trend, where the lift-drag ratio is decreasing for increasing flapwise stiffness and relatively independent of airfoil design, but where the design lift coefficient is varying depending on the design philosophy. To complete the analysis, also the edgewise and torsional stiffness were analyzed, where the torsional stiffness followed the same trend as the flapwise stiffness and the edgewise stiffness was somewhat more scattered, but with an overall trend of a reduction in the design lift coefficient and lift-drag ratio as a function of edgewise stiffness.

Acknowledgements
The present work was funded by the Danish Energy Agency in the project "Light Rotor", EUDP 64010-0107 and co-funded by DTU Wind Energy and Vestas.

References

[1] Fuglsang P, Bak C 2004 Development of the Risø wind turbine airfoils. *Wind Energy*, 7:145-162.
[2] Bak C.,Andersen P B, Madsen H A, Gaunaa M, Fuglsang P, Bove S 2008 Design and verification of airfoils resistant to surface contamination and turbulence intensity *AIAA 2008–7050, 26th AIAA Applied Aerodyn. Conf.18–21 August 2008, Honolulu,Hawaii*
[3] Timmer WA, van Rooij R P J O M 2003 Summary of the delft university wind turbine dedicated airfoils. *Proc. AIAA-2003-0352*.
[4] Tangler J L, Somers D M 1995 NREL airfoil families for hawt's. *Proc. WINDPOWER'95, Washington D.C.*, pages 117-123.
[5] Bak C, Gaunaa M, Antoniou I 2007 Performance of the Risø-B1 Airfoil Family for Wind Turbines, *Wind Energy Colloquium, Proceedings of the Euromech , Joachim Peinke, Peter Schaumann and Stephan Barth (Eds.), Springer-Verlag Berlin Heidelberg*
[6] Abbot I H, von Doenhoff A E 1959 Theory of wing sections: including a summary of airfoil data, *New York, Dover publications Inc.*, 693 p.
[7] Drela M 1989 XFOIL, An Analysis and Design system for Low Reynolds Number Airfoils. Low Reynolds Number Aerodynamics, *volume 54. In Springer- Verlag Lec*. Notes in Eng.
[8] Björk A 1990 Coordinates and calculations for the ffa-w1-xxx, ffa-w2-xxx and ffa-w3-.xxx series of airfoils for horizontal axis wind turbines, *FFA TN 1990-15, FFA, Stockholm, Sweden*.
[9] Fuglsang P, Dahl K S 1997 Multipoint optimization of thick high lift airfoil for wind turbines. *Proc. EWEC97, Dublin, Ireland*, pages 468-471.
[10] van Rooij R P J O M, Timmer W A 2003 Roughness Sensitivity Considerations for Thick Rotor Blade Airfoils, *Transactions of the ASME, Vol. 125*, November
[11] Døssing M 2011 Optimization of wind turbine rotors - using advanced aerodynamic and aeroelastic models and numerical optimization, *Risø-PhD-69(EN) , May, Risø National Laboratory for Sustainable Energy*
[12] Bak C 2013 Aerodynamic design of wind turbine rotors, in *Advances in wind turbine blade design and materials edited by Povl Brøndsted and Rogier Nijssen, Woodhead Publishing, ISBN 978 0 85709 426 1*